APPENDIX 2: MATHEMATICAL FOUNDATIONS OF LINEAR ELASTIC FRACTURE MECHANICS

(Selected Results)

A2.1 PLANE ELASTICITY

This section catalogs the governing equations from which linear fracture mechanics is derived. The reader is encouraged to review the basis of these relationships by consulting one of the many textbooks on elasticity theory.[3]

The equations that follow are simplifications of more general relationships in elasticity and are subject to the following restrictions:

- Two-dimensional stress state (plane stress or plane strain).
- Isotropic material.
- Quasistatic, isothermal deformation.
- Body forces are absent from the problem. (In problems where body forces are present, a solution can first be obtained in the absence of body forces, and then modified by superimposing the body forces.)

Imposing these restrictions simplifies crack problems considerably, and permits closed-form solutions in many cases.

The governing equations of plane elasticity are given below for rectangular Cartesian coordinates. Section A2.1.2 lists the same relationships in terms of polar coordinates.

A2.1.1 Cartesian Coordinates

Strain-displacement relationships:

$$\varepsilon_{xx} = \frac{\partial u_x}{\partial x} \varepsilon_{yy} = \frac{\partial u_y}{\partial y} \varepsilon_{xy} = \frac{1}{2}\left(\frac{\partial u_x}{\partial y} + \frac{\partial u_y}{\partial x}\right) \tag{A2.1}$$

where x and y are the horizontal and vertical coordinates, respectively, ε_{xx}, ε_{yy}, etc. are the strain components, and u_x and u_y are the displacement components.

---

[3] Appendix 2 is intended only for more advanced readers, who have at least taken one graduate-level course in the theory of elasticity.

Stress-strain relationships:

1. Plane strain.

$$\sigma_{xx} = \frac{E}{(1+\nu)(1-2\nu)}[(1-\nu)\varepsilon_{xx} + \nu\varepsilon_{yy}]$$

$$\sigma_{yy} = \frac{E}{(1+\nu)(1-2\nu)}[(1-\nu)\varepsilon_{yy} + \nu\varepsilon_{xx}]$$

$$\tau_{xy} = 2\mu\varepsilon_{xy} = \frac{E}{1+\nu}\varepsilon_{xy} \qquad \text{(A2.2)}$$

$$\sigma_{zz} = \nu(\sigma_{xx} + \sigma_{yy})$$

$$\varepsilon_{zz} = \varepsilon_{xz} = \varepsilon_{yz} = \tau_{xz} = \tau_{yz} = 0$$

where σ and τ are the normal and shear stress components, respectively, E is Young's modulus, μ is the shear modulus, and υ is Poisson's ratio.

2. Plane stress.

$$\sigma_{xx} = \frac{E}{1-\nu^2}[\varepsilon_{xx} + \nu\varepsilon_{yy}]$$

$$\sigma_{yy} = \frac{E}{1-\nu^2}[\varepsilon_{yy} + \nu\varepsilon_{xx}]$$

$$\tau_{xy} = 2\mu\varepsilon_{xy} = \frac{E}{1+\nu}\varepsilon_{xy} \qquad \text{(A2.3)}$$

$$\varepsilon_{zz} = \frac{-\upsilon}{1-\upsilon}(\varepsilon_{xx} + \varepsilon_{yy})$$

$$\sigma_{zz} = \varepsilon_{xz} = \varepsilon_{yz} = \tau_{xz} = \tau_{yz} = 0$$

Equilibrium equations:

$$\frac{\partial\sigma_{xx}}{\partial x} + \frac{\partial\tau_{xy}}{\partial y} = 0 \qquad \frac{\partial\sigma_{yy}}{\partial y} + \frac{\partial\tau_{xy}}{\partial x} = 0 \qquad \text{(A2.4)}$$

Compatibility equation:

$$\nabla^2(\sigma_{xx} + \sigma_{yy}) = 0 \qquad \text{(A2.5)}$$

where

$$\nabla^2 = \frac{\partial^2}{\partial x^2} + \frac{\partial^2}{\partial y^2}$$

Airy stress function:

For a two-dimensional continuous elastic medium, there exists a function $\Phi(x,y)$ from which the stresses can be derived:

$$\sigma_{xx} = \frac{\partial^2\Phi}{\partial y^2} \qquad \sigma_{yy} = \frac{\partial^2\Phi}{\partial x^2} \qquad \tau_{xy} = -\frac{\partial^2\Phi}{\partial x\partial y} \qquad \text{(A2.6)}$$

where Φ is the Airy stress function. The equilibrium and compatibility equations are automatically satisfied if Φ has the following property:

$$\frac{\partial^4\Phi}{\partial x^4} + 2\frac{\partial^4\Phi}{\partial x^2\partial y^2} + \frac{\partial^4\Phi}{\partial y^4} = 0$$

or

$$\nabla^2\nabla^2\Phi = 0 \qquad \text{(A2.7)}$$

A2.1.2 Polar Coordinates

Strain-displacement relationships:

$$\varepsilon_{rr} = \frac{\partial u_r}{\partial r} \qquad \varepsilon_{\theta\theta} = \frac{u_r}{r} + \frac{1}{r}\frac{\partial u_\theta}{\partial\theta} \qquad \varepsilon_{r\theta} = \frac{1}{2}\left(\frac{1}{r}\frac{\partial u_r}{\partial\theta} + \frac{\partial u_\theta}{\partial r} - \frac{u_\theta}{r}\right) \qquad \text{(A2.8)}$$

where u_r and u_θ are the radial and tangential displacement components, respectively.

Stress-strain relationships:

The stress-strain relationships in polar coordinates can be obtained by substituting r and θ for x and y in Eqs. (A2.2) and (A2.3). For example, the radial stress is given by

$$\sigma_{rr} = \frac{E}{(1+\nu)(1-2\nu)}[(1-\nu)\varepsilon_{rr} + \nu\varepsilon_{\theta\theta}] \qquad \text{(A2.9a)}$$

for plane strain, and

$$\sigma_{rr} = \frac{E}{1-\nu^2}[\varepsilon_{rr} + \nu\varepsilon_{\theta\theta}] \tag{A2.9b}$$

for plane stress.

Equilibrium equations:

$$\frac{\partial\sigma_{rr}}{\partial r} + \frac{1}{r}\frac{\partial\tau_{r\theta}}{\partial\theta} + \frac{\sigma_{rr}-\sigma_{\theta\theta}}{r} = 0$$

$$\frac{1}{r}\frac{\partial\sigma_{\theta\theta}}{\partial\theta} + \frac{\partial\tau_{r\theta}}{\partial r} + \frac{2\tau_{r\theta}}{r} = 0 \tag{A2.10}$$

Compatibility equation:

$$\nabla^2(\sigma_{rr} + \sigma_{\theta\theta}) = 0 \tag{A2.11}$$

where

$$\nabla^2 = \frac{\partial^2}{\partial r^2} + \frac{1}{r}\frac{\partial}{\partial r} + \frac{1}{r^2}\frac{\partial^2}{\partial\theta^2}$$

Airy stress function:

$$\nabla^2\nabla^2\Phi = 0 \tag{A2.12}$$

where $\Phi = \Phi(r,\theta)$ and

$$\sigma_{rr} = \frac{1}{r^2}\frac{\partial^2\Phi}{\partial\theta^2} + \frac{1}{r}\frac{\partial\Phi}{\partial r} \qquad \sigma_{\theta\theta} = \frac{\partial^2\Phi}{\partial r^2} \qquad \tau_{rq} = -\frac{1}{r}\frac{\partial^2\Phi}{\partial r\partial\theta} + \frac{1}{r^2}\frac{\partial\Phi}{\partial\theta} \tag{A2.13}$$

A2.2 CRACK GROWTH INSTABILITY ANALYSIS

Figure 2.12 schematically illustrates the general case of a cracked structure with finite system compliance, C_M. The structure is held at a fixed remote displacement, Δ_T given by

$$\Delta_T = \Delta + C_M P \tag{A2.14}$$

where Δ is the local load line displacement and P is the applied load. Differentiating Eq. (A2.14) gives

$$d\Delta_T = \left(\frac{\partial\Delta}{\partial a}\right)_P da + \left(\frac{\partial\Delta}{\partial P}\right)_a dP + C_M dP = 0 \tag{A2.15}$$

assuming Δ depends only on load and crack length. We can make this same assumption about the energy release rate:

$$d\mathcal{G} = \left(\frac{\partial\mathcal{G}}{\partial a}\right)_P da + \left(\frac{\partial\mathcal{G}}{\partial P}\right)_a dP \tag{A2.16}$$

Dividing both sides of Eq. (A2.16) by da and fixing Δ_T yields

$$\left(\frac{d\mathcal{G}}{da}\right)_{\Delta_T} = \left(\frac{\partial\mathcal{G}}{\partial a}\right)_P + \left(\frac{\partial\mathcal{G}}{\partial P}\right)_a \left(\frac{dP}{da}\right)_{\Delta_T} \tag{A2.17}$$

which, upon substitution of Eq. (A2.15), leads to

$$\left(\frac{d\mathcal{G}}{da}\right)_{\Delta_T} = \left(\frac{\partial\mathcal{G}}{\partial a}\right)_P - \left(\frac{\partial\mathcal{G}}{\partial P}\right)_a \left(\frac{\partial\Delta}{\partial a}\right)_P \left[C_m + \left(\frac{\partial\Delta}{\partial P}\right)_a\right]^{-1} \tag{A2.18}$$

A virtually identical expression for the J integral (Eq. 3.52) can be derived by assuming J depends only on P and a, and expanding dJ into its partial derivatives.

Under dead-loading conditions, $C_M = \infty$, and all but the first term in Eq. (A2.18) vanish. Conversely, $C_M = 0$ corresponds to an infinitely stiff system, and Eq. (A2.18) reduces to the pure displacement control case.

A2.3 CRACK TIP STRESS ANALYSIS

A variety of techniques are available for analyzing stresses in cracked bodies. This section focuses on two early approaches developed by Williams [11,35] and Westergaard [8]. These two analyses are complementary; the Williams approach considers the local crack tip fields under generalized in-plane loading, while Westergaard provided a means for connecting the local fields to global boundary conditions in certain configurations.

Space limitations preclude listing every minute step in each derivation. Moreover, stress, strain, and displacement distributions are not derived for all modes of loading. The derivations that follow serve as illustrative examples. The reader who is interested in further details should consult the original references.

A2.3.1 Generalized In-Plane Loading

Williams [11,35] was the first to demonstrate the universal nature of the $1/\sqrt{r}$ singularity for elastic crack problems, although Inglis [1], Westergaard [8] and Sneddon [10] had earlier obtained this result in specific configurations. Williams actually began by considering stresses at the corner of a plate with various boundary conditions and included angles; a crack is a special case where the included angle of the plate corner is 2π and the surfaces are traction free (Fig. A2.1).

For the configuration shown in Fig. A2.1(b), Williams postulated the following stress function:

$$\Phi = r^{\lambda+1}[c_1 \sin(\lambda+1)\theta^* + c_2 \cos(\lambda+1)\theta^* + c_3 \sin(\lambda-1)\theta^* + c_4 \cos(\lambda-1)\theta^*] = r^{\lambda+1}\phi(\theta^*,\lambda) \tag{A2.19}$$

where c_1, c_2, c_3, and c_4 are constants, and θ^* is defined in Fig. A2.1(b). Invoking Eq. (A2.13) gives the following expressions for the stresses:

$$\sigma_{rr} = r^{\lambda-1}[F''(\theta^*) + (\lambda+1)F(\theta^*)]$$

$$\sigma_{\theta\theta} = r^{\lambda-1}[\lambda(\lambda+1)F(\theta^*)] \tag{A2.20}$$

$$\tau_{r\theta} = r^{\lambda-1}[-\lambda F'(\theta^*)]$$

where the primes denote derivatives with respect to θ^*. Williams also showed that Eq. (A2.19) implies that the displacements vary with r^{λ}. In order for displacements to be finite in all regions of the body, λ must be > 0. If the crack faces are traction free, $\sigma_{\theta\theta}(0) = \sigma_{\theta\theta}(2\pi) = \tau_{r\theta}(0) = \tau_{r\theta}(2\pi) = 0$, which implies the following boundary conditions:

$$F(0) = F(2\pi) = F'(0) = F'(2\pi) = 0 \tag{A2.21}$$

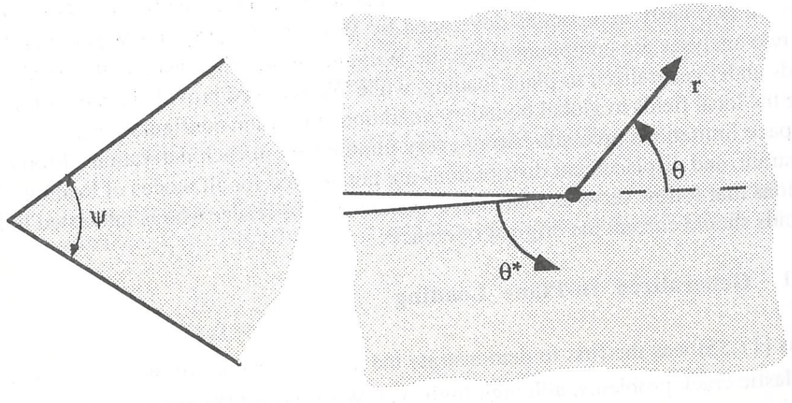

(a) Plate corner with included angle y. (b) Special case of a sharp crack.

FIGURE A2.1 Plate corner configuration analyzed by Williams [35]. A crack is formed when $\psi = 2\pi$.

Assuming the constants in Eq. (A2.19) are nonzero in the most general case, the boundary conditions can only be satisfied when $\sin(2\pi\lambda)=0$. Thus

$$\lambda = \frac{n}{2}, \quad \text{where n = 1, 2, 3, . . .}$$

There are an infinite number of λ values that satisfy the boundary conditions; the most general solution to a crack problem, therefore, is a polynomial of the form

$$\Phi = \sum_{n=1}^{N}\left(r^{\frac{n}{2}+1}F(\theta^*,\tfrac{n}{2})\right) \tag{A2.22}$$

and the stresses are given by

$$\sigma_{ij} = \frac{\Gamma_{ij}\left(\theta^*,-\frac{1}{2}\right)}{\sqrt{r}} + \sum_{m=0}^{M}\left(r^{m/2}\Gamma_{ij}(\theta^*,m)\right) \tag{A2.23}$$

where Γ is a function that depends on F and its derivatives. The order of the stress function polynomial, N, must be sufficient to model the stresses in all regions of the body. When $r \to 0$, the first term in Eq. (A2.23) approaches infinity, while the higher order terms remain finite (when $m = 0$) or approach zero (for $m > 0$). Thus the higher order terms are negligible close to the crack tip, and stress exhibits an $1/\sqrt{r}$ singularity. Note that this result was obtained without assuming a specific configuration; thus it can be concluded that the inverse square-root singularity is universal for cracks in isotropic elastic media.

Further evaluation of Eqs. (A2.19) and (A2.20) with the appropriate boundary conditions reveals the precise nature of the function Γ. Recall that Eq. (A2.19) contains four, as yet unspecified, constants; by applying Eq. (A2.21), it is possible to eliminate two of these constants, resulting in

$$\Phi(r,\theta) = r^{n/2+1}\left\{c_3\left[\sin\left(\frac{n}{2}-1\right)\theta^* - \frac{n-2}{n+2}\sin\left(\frac{n}{2}+1\right)\theta^*\right] + c_4\left[\cos\left(\frac{n}{2}-1\right)\theta^* - \cos\left(\frac{n}{2}+1\right)\theta^*\right]\right\} \tag{A2.24}$$

for a given value of n. For crack problems it is more convenient to express the stress function in terms of, θ, the angle from the symmetry plane (Fig. A2.1). Substituting $\theta = \theta^* - \pi$ into Eq. (A2.24) yields, after some algebra, the following stress function for the first few values of n:

$$\Phi(r,\theta) = r^{3/2}\left[s_1\left(-\cos\frac{\theta}{2} - \frac{1}{3}\cos\frac{3\theta}{2}\right) + t_1\left(-\sin\frac{\theta}{2} - \sin\frac{3\theta}{2}\right)\right]$$

where *Re* and *Im* denote real and imaginary parts of the function, respectively, and the bars over Z represent integrations with respect to z; i.e.,

$$\bar{\bar{Z}} = \frac{d\bar{\bar{Z}}}{dz} \qquad \text{and} \qquad Z = \frac{d\bar{Z}}{dz}$$

Applying Eq. (A2.6) gives

$$\begin{aligned} \sigma_{xx} &= \mathrm{Re}\, Z - y\,\mathrm{Im}\, Z' \\ \sigma_{yy} &= \mathrm{Re}\, Z + y\,\mathrm{Im}\, Z' \\ \tau_{xy} &= -y\,\mathrm{Re}\, Z' \end{aligned} \tag{A2.31}$$

Note that the imaginary part of the stresses vanishes when y=0. In addition, the shear stress vanishes when $y = 0$, implying that the crack plane is a principal plane. Thus the stresses are symmetric about $\theta = 0$ and Eq. (A2.31) implies Mode I loading.

The Westergaard stress function, in its original form, is suitable for solving a limited range of Mode I crack problems. Subsequent modifications [36-39] generalized the Westergaard approach to be applicable to a wider range of cracked configurations.

Consider a through crack in an infinite plate subject to biaxial remote tension (Fig. A2.2). If the origin is defined at the center of the crack, the Westergaard stress function is given by

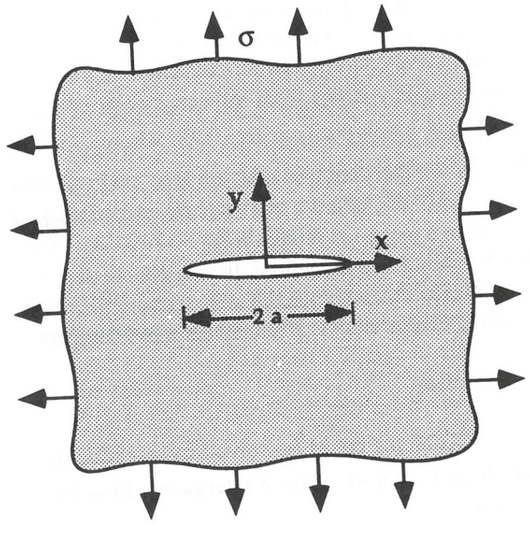

FIGURE A2.2 Through-thickness crack in an infinite plate loaded in biaxial tension.

$$Z(z) = \frac{\sigma z}{\sqrt{z^2 - a^2}} \tag{A2.32}$$

where σ is the remote stress and a is the half crack length, as defined in Fig. A2.2. Consider the crack plane where y=0. For $-a < x < a$, Z is pure imaginary, while Z is real for $|x| > |a|$. The normal stresses on the crack plane are given by

$$\sigma_{xx} = \sigma_{yy} = \mathrm{Re}\, Z = \frac{\sigma x}{\sqrt{x^2 - a^2}} \tag{A2.33}$$

Let us now consider the horizontal distance from each crack tip, $x^* = x\text{-}a$; Eq. (A2.33) becomes

$$\sigma_{xx} = \sigma_{yy} = \frac{\sigma\sqrt{a}}{\sqrt{2x^*}} \tag{A2.34}$$

for $x^* << a$. Thus the Westergaard approach leads to the expected inverse square-root singularity. One advantage of this analysis is that it relates the local stresses to the global stress and crack size. From Eq. (A2.28), the stresses on the crack plane (θ=0) are given by

$$\sigma_{rr} = \sigma_{\theta\theta} = \sigma_{xx} = \sigma_{yy} = \frac{K_I}{\sqrt{2\pi x^*}} \tag{A2.35}$$

Comparing Eqs. (A2.34) and (A2.35) gives

$$K_I = \sigma\sqrt{\pi a} \tag{A2.36}$$

for the configuration in Fig. A2.2. Note that $\sqrt{\pi}$ appears in Eq. (A2.36) because K was originally defined in terms of the energy release rate; an alternative definition of stress intensity might be

$$\sigma_{yy}(\theta = 0) = \frac{K_I^*}{\sqrt{2x^*}} \quad \text{where} \quad K_I^* = \sigma\sqrt{a} \quad \text{for the plate in Fig. A2.2.}$$

Substituting Eq. (A3.36) into Eq. (A2.32) results in an expression of the Westergaard stress function in terms of K_I:

$$Z(z^*) = \frac{K_I}{\sqrt{2\pi z^*}} \tag{A2.37}$$

where $z^* = z\text{-}a$. It is possible to solve for the singular stresses at other angles by making the following substitution in Eq. (A2.37):

$$z^* = re^{i\theta}$$

where

$$r^2 = (x-a)^2 + y^2 \qquad \text{and} \qquad \theta = \tan^{-1}\left(\frac{y}{x-a}\right)$$

which leads to

$$\sigma_{xx} = \frac{K_I}{\sqrt{2\pi r}}\cos\left(\frac{\theta}{2}\right)\left[1-\sin\left(\frac{\theta}{2}\right)\sin\left(\frac{3\theta}{2}\right)\right]$$

$$\sigma_{yy} = \frac{K_I}{\sqrt{2\pi r}}\cos\left(\frac{\theta}{2}\right)\left[1+\sin\left(\frac{\theta}{2}\right)\sin\left(\frac{3\theta}{2}\right)\right] \qquad \text{(A2.38)}$$

$$\tau_{xy} = \frac{K_I}{\sqrt{2\pi r}}\cos\left(\frac{\theta}{2}\right)\sin\left(\frac{\theta}{2}\right)$$

assuming $r>>a$. Equation (A2.38) is equivalent to Eq. (A2.28), except that the latter is expressed in terms of polar coordinates.

Westergaard published the following stress function for an array of collinear cracks in a plate in biaxial tension (Fig 2.21):

$$Z(z) = \frac{\sigma}{\left\{1-\left[\frac{\sin\left(\frac{\pi a}{2W}\right)}{\sin\left(\frac{\pi z}{2W}\right)}\right]^2\right\}^{1/2}} \qquad \text{(A2.39)}$$

where a is the half crack length and $2W$ is the spacing between the crack centers. The stress intensity for this case is given in Eq. (2.45); early investigators used this solution to approximate the behavior of center cracked tensile panel with finite width.

Irwin [9] published stress functions for several additional configurations, including a pair of crack opening forces located a distance X from the crack center (Fig. 2.30):

$$Z(z) = \frac{Pa}{p(z-X)z}\sqrt{\frac{1-(X/a)^2}{1-(a/z)^2}} \qquad \text{(A2.40)}$$

where P is the applied force. When there are matching forces at $\pm X$, the appropriate stress function can be obtained by superposition:

$$Z(z) = \frac{2Pa}{\pi(z^2-X^2)}\sqrt{\frac{1-(X/a)^2}{1-(a/z)^2}} \qquad \text{(A2.41)}$$

In each case, the stress function can be expressed in the form of Eq. (A2.37) and the near tip stresses are given by Eq. (A2.38). This is not surprising, since all of the above cases are pure Mode I and the Williams analysis showed that the inverse square root singularity is universal.

For plane strain conditions, the in-plane displacements are related to the Westergaard stress function as follows:

$$u_x = \frac{1}{2\mu}[(1-2\nu)\,\mathrm{Re}\,\bar{Z} - y\,\mathrm{Im}\,Z]$$

$$u_y = \frac{1}{2\mu}[2(1-\nu)\,\mathrm{Im}\,\bar{Z} - y\,\mathrm{Re}\,Z] \qquad \text{(A2.42)}$$

For the plate in Fig. A2.2, the crack opening displacement is given by

$$2u_y = \frac{1-\nu}{\mu}\mathrm{Im}\,\bar{Z} = \frac{2(1-\nu^2)}{E}\mathrm{Im}\,\bar{Z} = \frac{4(1-\nu^2)\sigma}{E}\sqrt{a^2-x^2} \qquad \text{(A2.43a)}$$

assuming plane strain, and

$$2u_y = \frac{4\sigma}{E}\sqrt{a^2-x^2} \qquad \text{(A2.43b)}$$

for plane stress. Eq. (A2.43) predicts that a through crack forms an elliptical opening profile when subjected to tensile loading.

The near-tip displacements can be obtained by inserting Eq. (A2.37) into Eq. (A2.42):

$$u_x = \frac{K_I}{2\mu}\sqrt{\frac{r}{2\pi}}\cos\left(\frac{\theta}{2}\right)\left[\kappa-1+2\sin^2\left(\frac{\theta}{2}\right)\right]$$

$$u_y = \frac{K_I}{2\mu}\sqrt{\frac{r}{2\pi}}\sin\left(\frac{\theta}{2}\right)\left[\kappa+1-2\cos^2\left(\frac{\theta}{2}\right)\right] \qquad \text{(A2.44)}$$

for $r << a$, where

$$\kappa = 3-4\nu \qquad \text{for plane strain}$$

and

$$k = \frac{3-\nu}{1+\nu} \qquad \text{for plane stress} \qquad \text{(A2.45)}$$

Although the original Westergaard approach correctly describes the singular Mode I stresses in certain configurations, it is not sufficiently general to apply to all Mode I problems; this shortcoming has prompted various modifications to the Westergaard stress function. Irwin [36] noted that photoelastic fringe patterns observed by Wells and Post [40] on center cracked panels did not match the shear strain contours predicted by the Westergaard solution. Irwin achieved good agreement between theory and experiment by subtracting a uniform horizontal stress:

$$\sigma_{xx} = \mathrm{Re}\, Z - y\,\mathrm{Im}\, Z' - \sigma_{oxx} \tag{A2.46}$$

where σ_{oxx} depends on the remote stress. The other two stress components remain the same as in Eq. (A2.31). Subsequent analyses have revealed that when a center cracked panel is loaded in uniaxial tension, a transverse compressive stress develops in the plate. Thus Irwin's modification to the Westergaard solution has a physical basis in the case of a center cracked panel[4]. Equation (A2.46) has been used to interpret photoelastic fringe patterns in a variety of configurations.

Sih [37] provided a theoretical basis for the Irwin modification. A stress function for Mode I must lead to zero shear stress on the crack plane. Sih showed that the Westergaard function was more restrictive than it needed to be, and was thus unable to account for all situations. Sih generalized the Westergaard approach by applying a complex potential formulation for the Airy stress function [41]. He imposed the condition $\tau_{xy} = 0$ at y=0, and showed that the stresses could be expressed in terms of a new function $f(z)$:

$$\begin{aligned}
\sigma_{xx} &= 2\,\mathrm{Re}\,\phi'(z) - 2y\,\mathrm{Im}\,\phi''(z) - A \\
\sigma_{yy} &= 2\,\mathrm{Re}\,\phi'(z) + 2y\,\mathrm{Im}\,\phi''(z) + A \\
\tau_{xy} &= 2y\,\mathrm{Re}\,\phi''(z)
\end{aligned} \tag{A2.47}$$

where A is a real constant. Equation (A2.47) is equivalent to the Irwin modification of the Westergaard approach if

$$2\phi'(z) = Z(z) - A \tag{A2.48}$$

Substituting Eq. (A2.48) into Eq. (A2.47) gives

$$\begin{aligned}
\sigma_{xx} &= \mathrm{Re}\, Z - y\,\mathrm{Im}\, Z' - 2A \\
\sigma_{yy} &= \mathrm{Re}\, Z + y\,\mathrm{Im}\, Z'
\end{aligned} \tag{A2.49}$$

[4]Recall that the stress functions in Eqs. (2.32) and (2.39) are strictly valid only for biaxial loading. Although this restriction was not imposed in Westergaard's original work, a transverse tensile stress is necessary in order to cancel with $-\sigma_{oxx}$. However, the transverse stresses, whether compressive or tensile, do not affect the singular term; thus the stress intensity factor is the same for uniaxial and biaxial tensile loading and is given by Eq. (A2.36).

$$\tau_{xy} = -y\,\mathrm{Re}\, Z'$$

Comparing Eq. (A2.49) with Eqs. (A2.31) and (A2.46), it is obvious that the Sih and Irwin modifications are equivalent and $2A=\sigma_{oxx}$.

Sanford [39] showed that the Irwin-Sih approach is still too restrictive, and he proposed replacing A with a complex function $\eta(z)$:

$$2\phi'(z) = Z(z) - \eta(z) \tag{A2.50}$$

The modified stresses are given by

$$\begin{aligned}
\sigma_{xx} &= \mathrm{Re}\, Z - y\,\mathrm{Im}\, Z' + y\,\mathrm{Im}\,\eta' - 2\,\mathrm{Re}\,\eta \\
\sigma_{yy} &= \mathrm{Re}\, Z + y\,\mathrm{Im}\, Z' + y\,\mathrm{Im}\,\eta' \\
\tau_{xy} &= -y\,\mathrm{Re}\, Z' + y\,\mathrm{Re}\,\eta' + \mathrm{Im}\,\eta
\end{aligned} \tag{A2.51}$$

Equation (A2.51) represents the most general form of Westergaard-type stress functions. When $\eta(z)=a$ real constant for all z, Eq. (A2.51) reduces to the Irwin-Sih approach, while Eq. (A2.51) reduces to the original Westergaard solution when $\eta(z) = 0$ for all z.

The function η can be represented as a polynomial of the form

$$\eta(z) = \sum_{m=0}^{M} \alpha_m z^{m/2} \tag{A2.52}$$

Combining Eqs. (A2.37), (A2.50), and (A2.52) and defining the origin at the crack tip gives

$$2\phi' = \frac{K_I}{\sqrt{2\pi z}} - \sum_{m=0}^{M} \alpha_m z^{m/2} \tag{A2.53}$$

which is consistent with the Williams [11,35] asymptotic expansion.

A2.4 ELLIPTICAL INTEGRAL OF THE SECOND KIND

The solution of stresses in the vicinity of elliptical and semielliptical cracks in elastic solids [10,42] involves an elliptic integral of the second kind:

$$\Psi = \int_0^{\pi/2} \sqrt{1 - \frac{c^2 - a^2}{c^2} \sin^2\phi}\, d\phi \tag{A2.54}$$

where $2c$ and $2a$ are the major and minor axes of the elliptical flaw, respectively. Series expansion of Eq. (A2.54) gives

$$\Psi = \frac{\pi}{2}\left[1 - \frac{1}{4}\frac{c^2 - a^2}{c^2} - \frac{3}{64}\left(\frac{c^2 - a^2}{c^2}\right)^2 - \ldots\right] \tag{A2.55}$$

Most stress intensity solutions for elliptical and semi-ellipical cracks in the published literature are written in terms of a flaw shape parameter, Q, which can be approximated by

$$Q = \Psi^2 \approx 1 + 1.464\left(\frac{a}{c}\right)^{1.65} \tag{A2.56}$$

3. ELASTIC-PLASTIC FRACTURE MECHANICS

Linear elastic fracture mechanics (LEFM) is valid only as long as nonlinear material deformation is confined to a small region surrounding the crack tip. In many materials, it is virtually impossible to characterize the fracture behavior with LEFM, and an alternative fracture mechanics model is required.

Elastic-plastic fracture mechanics applies to materials that exhibit time-independent, nonlinear behavior (i.e., plastic deformation). Two elastic-plastic parameters are introduced in this chapter: the crack tip opening displacement (*CTOD*) and the *J* contour integral. Both parameters describe crack tip conditions in elastic-plastic materials, and each can be used as a fracture criterion. Critical values of *CTOD* or *J* give nearly size-independent measures of fracture toughness, even for relatively large amounts of crack tip plasticity. There are limits to the applicability of *J* and *CTOD*(Sections 3.5 & 3.6), but these limits are much less restrictive than the validity requirements of LEFM.

3.1 CRACK TIP OPENING DISPLACEMENT

When Wells [1] attempted to measure K_{Ic} values in a number of structural steels, he found that these materials were too tough to be characterized by LEFM. This discovery brought both good news and bad news: high toughness is obviously desirable to designers and fabricators, but Wells' experiments indicated that existing fracture mechanics theory was not applicable to an important class of materials. While examining fractured test specimens, Wells noticed that the crack faces had moved apart prior to fracture; plastic deformation blunted an initially sharp crack, as illustrated in Fig. 3.1. The degree of crack blunting increased in proportion to the toughness of the material. This observation led Wells to propose the opening at the crack tip as a measure of fracture toughness. Today, this parameter is known as the crack tip opening displacement (*CTOD*).

In his original paper, Wells [1] performed an approximate analysis that related *CTOD* to the stress intensity factor in the limit of small scale yielding. Consider a crack with a small plastic zone, as illustrated in Fig. 3.2. Irwin [2] showed that crack tip plasticity makes the crack behave as if it were slightly longer. Thus, we can estimate *CTOD* by solving for the displacement at the physical crack tip, assuming an effective crack length of $a+r_y$. From Table 2.2, the displacement r_y behind the effective crack tip is given by

$$u_y = \frac{\kappa + 1}{2\mu} K_I \sqrt{\frac{r_y}{2\pi}} \tag{3.1}$$

and the Irwin plastic zone correction for plane stress is